

Infrared safe perturbative approach to Yang-Mills correlatorsMatthieu Tissier¹ and Nicolás Wschebor²¹*Laboratoire de Physique Théorique de la Matière Condensée, Université Pierre et Marie Curie,
4 Place Jussieu 75252 Paris CEDEX 05, France*²*Instituto de Física, Facultad de Ingeniería, Universidad de la República, J. H. y Reissig 565, 11000 Montevideo, Uruguay*
(Received 13 May 2011; published 18 August 2011)

We investigate the 2-point correlation functions of Yang-Mills theory in the Landau gauge by means of a massive extension of the Faddeev-Popov action. This model is based on some phenomenological arguments and constraints on the ultraviolet behavior of the theory. We show that the running coupling constant remains finite at all energy scales (no Landau pole) for $d > 2$ and argue that the relevant parameter of perturbation theory is significantly smaller than 1 at all energies. Perturbative results at low orders are therefore expected to be satisfactory and we indeed find a very good agreement between one-loop correlation functions and the lattice simulations, in three and four dimensions. Dimension-2 is shown to play the role of an upper critical dimension, which explains why the lattice predictions are qualitatively different from those in higher dimensions.

DOI: [10.1103/PhysRevD.84.045018](https://doi.org/10.1103/PhysRevD.84.045018)

PACS numbers: 12.38.-t, 11.10.Kk, 12.38.Aw, 12.38.Bx

I. INTRODUCTION

There is currently no fully satisfying covariant gauge fixing of non-Abelian gauge theories. The common Faddeev-Popov (FP) procedure is known to be invalid because of the Gribov ambiguity [1]: the gauge constraint (such as $\partial_\mu A_\mu^a = 0$ in the Landau gauge) has many solutions (Gribov copies) equivalent up to a gauge transformation. Taking into account this ambiguity would give nonperturbative contributions [typically of the form $\exp(-\text{const.}/g^2)$] that vanish at all orders of the perturbation theory. Consequently, the FP procedure is actually justified when studying high-energy phenomena and the perturbative predictions are in excellent agreement with the experiments. On the other range of the spectrum, when considering infrared (IR) properties, the perturbative analysis extracted from the FP procedure is inconsistent because the coupling becomes large. The coupling is found to diverge at a finite energy scale (known as a Landau pole) but of course this prediction is out of the range of validity of perturbation theory. There are two possible explanations of the failure of the perturbative predictions of the FP procedure. Either the coupling indeed reaches large values (but this seems to be at odds with the lattice simulation results) or some nonperturbative effects, such as the Gribov ambiguity, invalidate the FP procedure itself.

In fact, we can avoid fixing the gauge by simulating gauge invariant quantities on the lattice and most of the IR studies are done in this way. However it would be convenient to have some analytic (or semianalytic) predictions in that regime, which seem to require one to fix the gauge (see however [2–4]), and therefore to take into account the Gribov ambiguity.

Several analytic methods have been considered in order to access the IR properties. The most developed is based on the Schwinger-Dyson (SD) equations [5–16], which

consist of an infinite set of coupled equations for the vertex functions. In order to make predictions, it is necessary to truncate in some way this infinite set. Different schemes have been proposed but most of them consider the equations for the 2-point functions with an ansatz for the 3- and 4-point functions. (Most of the analyses have been done in the Landau gauge and we restrict the discussion to this gauge in the rest of the paper.) This leads to some predictions on the behavior of the ghost and gluon propagators and two types of solutions have been found. In the so-called scaling solution [5–9,15], both propagators have a power-law behavior in the IR, the ghost propagator is more singular than the bare one, and the gluon propagator approaches zero in that limit. The exponents governing these two power-laws are not independent. In the so-called decoupling solution (or massive solution) [9–14,16], the gluon propagator goes to a constant in the IR, and the ghost propagator is as singular as in the bare theory.

These correlation functions were also studied in the framework of the nonperturbative renormalization group (NPRG) equation [17,18]. Again, one has to make some truncations in an infinite set of coupled equations [15,19,20]. The results again depend on the approximation scheme, but seem to be consistent with the scaling solution.

A third approach, known as the Gribov-Zwanziger (GZ) model [1,21,22], relies more specifically on the influence of the Gribov copies. By introducing several auxiliary fields, it is possible to restrict effectively the functional integration on the gluon field to the first Gribov region, where the FP operator is positive-definite. It was originally expected that this restriction would give an unambiguous gauge fixing but it was later realized that many copies of some field configuration were present within the first Gribov region [23]. This procedure significantly reduces the number of Gribov copies but unfortunately not to a single one. The Gribov ambiguity is therefore still present

in this model. In the first implementations of the GZ model, the predictions for the propagators were consistent with the scaling solution. More recently a refined version of this model was introduced [24], that takes into account the appearance of some condensates. The results are then consistent with the massive solution of SD equations.

The results obtained in the SD approach triggered a large activity from the lattice community. Since the predictions of the SD approaches are mostly for gauge dependent quantities, it was necessary to implement a gauge-fixing procedure in the lattice, at odds with usual simulations. One of the merits of the precursor work of Alkofer and von Smekal [5,6] was to discard very singular solutions found previously for the gluon propagator and this was confirmed by the lattice simulations. However, a broad consensus on the details of the simulation results in $d = 3$ and 4 was achieved only recently, mainly through large lattice simulations [25–29]. It is now well established that in these dimensions, the simulations support the massive solution. The $d = 2$ case is different in this respect [26,30] and is well described by the scaling solution and the explanation of this difference is still unclear (see however [31]).

Recently [32], we proposed an alternative to the analytical methods described above. Its motivation relies on the fact that we do not have so far a fully justified covariant gauge-fixing procedure that can be handled in analytical calculations. Ideally, we should try to construct such an unambiguous gauge-fixing procedure, but this is an extremely hard task. Alternatively, we propose to construct a model that uses, as a guiding principle, the behavior of correlation functions observed on the lattice and that respects as many important known properties of correlation functions as possible. More precisely, since the gluon propagator is observed to be massive in the lattice simulations (for $d > 2$), we propose to include this mass term directly at the bare level. (This corresponds to a particular case of the Curci-Ferrari model [33].) This modifies the theory in the IR but preserves the standard FP predictions for momenta $p \gg m$ at all orders of perturbation theory. In particular, the mass term does not spoil the renormalizability. This model reproduces at one-loop order with excellent precision the lattice predictions. We also showed that the spectral function of the gluons is not positive-definite, in agreement with other studies [6,34,35].

Our aims in the present article are the following. First, we give a detailed version of the calculations presented in [32], including some other one-loop calculations that were not presented in the previous work for lack of space. Second, we show that an appropriate renormalization scheme can be chosen that does not present a Landau pole in the IR. Third, we discuss in detail the size of higher loop corrections showing that, in fact, they seem to be rather small. This opens the door to perturbative calculations in QCD in the IR regime, with a huge number of possible applications. Fourth, we analyze the $d = 2$ case

and explain why in the present model it is very different from the $d > 2$ case.

The article is organized as follows. In Sec. II, we describe in detail the model and its general properties. In Sec. III, we present the one-loop perturbative calculation of the 2-point functions and compare our results with the lattice data in $d = 4$ and $d = 3$. In Sec. IV, we perform a renormalization group (RG) analysis of these propagators. We propose two different renormalization schemes, one of which is shown to be IR safe in the sense that it leads to no Landau pole in the IR. We compare the RG results with the lattice data in $d = 4$ and $d = 3$. In Sec. V, we discuss the $d = 2$ case. Some technical details are presented in two appendices.

II. THE MODEL

As said in the introduction, the FP action is not justified at a nonperturbative level. In this section, we present a modification of the FP action in the Landau gauge, based on phenomenological considerations. Our main guide is the observation that the gluon propagator tends to a finite positive value in the IR for $d > 2$. We propose to impose this property at the tree level by adding a mass term for the gluon in the FP action. We do not change the ghost sector since the ghost propagator is found to be IR divergent in the simulations. This may also be motivated by assuming that the shift symmetry $\bar{c} \rightarrow \bar{c} + \text{const.}$ is preserved beyond perturbation theory. Moreover, we do not want to modify interactions in the action so as to preserve the ultraviolet (UV) behavior of the theory and maintain the predictions of perturbative QCD (or gluodynamics) for momenta much larger than Λ_{QCD} . From this analysis it is clear that if we choose not to modify the field content of the theory, mass terms are the only local and renormalizable modifications of the FP action that do not affect the UV behavior of the model. If we restrict to local terms, the only other possible way to modify the action is to introduce new fields as done in the GZ model [1,21,22]. The origin of the appearance of the effective mass term in the IR is a complex problem and could be related with the Gribov ambiguity, with some kind of condensates (see for example [24,36,37]), or with other nonperturbative effects, but our phenomenological approach does not rely on which of these scenarios is valid.

This analysis leads us to consider the Landau-gauge FP Euclidean Lagrangian for pure gluodynamics, supplemented with a gluon mass term:

$$\mathcal{L} = \frac{1}{4}(F_{\mu\nu}^a)^2 + \partial_\mu \bar{c}^a (D_\mu c)^a + ih^a \partial_\mu A_\mu^a + \frac{m^2}{2}(A_\mu^a)^2, \quad (1)$$

where $(D_\mu c)^a = \partial_\mu c^a + gf^{abc}A_\mu^b c^c$ and the field strength $F_{\mu\nu}^a = \partial_\mu A_\nu^a - \partial_\nu A_\mu^a + gf^{abc}A_\mu^b A_\nu^c$ are expressed in terms of the coupling constant g , and the Latin indices correspond to the $SU(N)$ gauge group. The Lagrangian (1) corresponds to a particular case of the Curci-Ferrari

model [33]. At the tree level, the gluon propagator is massive and transverse in momentum space:

$$G_{\mu\nu}^{ab}(p) = \delta^{ab} P_{\mu\nu}^{\perp}(p) \frac{1}{p^2 + m^2}, \quad (2)$$

with $P_{\mu\nu}^{\perp}(p) = \delta_{\mu\nu} - p_{\mu}p_{\nu}/p^2$. It is interesting to note that the spectral density associated with the propagator (2) is positive and therefore there is no violation of positivity at the tree level. As discussed in [32], violations of positivity are present in the model but they are caused by fluctuations.

The gluon propagator observed in the lattice is not compatible at a quantitative level with the bare propagator (2) and we will show below that, by including the one-loop corrections, one obtains propagators for gluons and ghosts that are in impressive agreement with those obtained in the lattice in $d = 4$ and $d = 3$.

Let us mention that a mass term has been used to improve perturbative QCD results in order to reproduce the phenomenology of strong interactions [38–40]. Moreover, there are successful confinement models [41] that use actions including a gluon mass term. The difference with the model used in those works is that the Curci-Ferrari model is renormalizable, allowing one to perform perturbative calculations at any order. This also implies that the UV beta function identifies with the standard results of the FP procedure.

When analyzing the model described above, we must face the problem that the mass term breaks the Becchi-Rouet-Stora-Tyutin (BRST) symmetry [42,43] which is very important in the perturbative analysis. This symmetry has the form:

$$\begin{aligned} \delta A_{\mu}^a &= \eta (D_{\mu} c)^a, & \delta c^a &= -\eta \frac{g}{2} f^{abc} c^b c^c, \\ \delta \bar{c}^a &= \eta i h^a, & \delta i h^a &= 0, \end{aligned} \quad (3)$$

where η is a global Grassmanian parameter. The BRST symmetry is in general used to prove the renormalizability of the theory. However, the breaking of the BRST symmetry by the mass term is soft and therefore does not spoil renormalizability [33,44].

The BRST symmetry is also used to reduce the state space to the physical space, in which the theory is unitary (at least at the perturbative level) and breaking this symmetry spoils the standard proof of unitarity. This problem is actually common to essentially all methods that try to go beyond the standard perturbation theory (as the GZ model) because they all break the standard BRST symmetry. In this respect, the model considered here is not in a worse position than other approaches considered in the field. We must insist that this model is equivalent to the standard FP model in the UV limit $p \gg \Lambda_{\text{QCD}}$ if $m \sim \Lambda_{\text{QCD}}$. This means that in the domain of validity of standard perturbation theory, the model is as unitary as QCD. The unitarity of

the model in other momentum regimes is of course an important open problem, as it is in all gauge fixings in which standard BRST symmetry is broken.

The model with Lagrangian (1), as a particular case of the Curci-Ferrari model, has a pseudo-BRST symmetry (not nilpotent) that has the same form as the standard BRST (3) except for the h variation which reads $\delta i h^a = \eta m^2 c^a$. On top of this symmetry, the Lagrangian has all the standard symmetries of the FP action for the Landau gauge. This includes the shift in antighost $\bar{c} \rightarrow \bar{c} + \text{const.}$ a symplectic group [45], and four gauged supersymmetries [46,47]. As a consequence, the mass [48] and coupling constant [49] renormalization factors are fixed in terms of gluon and ghost field renormalizations. More precisely, by using the standard definition of renormalization factors (here the subscripts B denote bare quantities corresponding to their respective renormalized quantities without subscripts):

$$\begin{aligned} A_B^{a\mu} &= \sqrt{Z_A} A^{a\mu}, & c_B^a &= \sqrt{Z_c} c^a, & \bar{c}_B^a &= \sqrt{Z_{\bar{c}}} \bar{c}^a, \\ g_B &= Z_g g, & m_B^2 &= Z_{m^2} m^2, \end{aligned} \quad (4)$$

one can prove that the divergent part of the renormalization factors (or, similarly, the renormalization factors themselves in a $\overline{\text{MS}}$ scheme) verify the two nonrenormalization theorems [48,49]:

$$Z_g \sqrt{Z_A} Z_c = 1, \quad (5)$$

$$Z_{m^2} Z_A Z_c = 1. \quad (6)$$

These nonrenormalization theorems are particular cases of those found in the Curci-Ferrari model for any gauge parameter ξ , as proven recently [46,50]. The finite parts of renormalized vertices also verify nonrenormalization theorems, as will be discussed below, but their explicit forms depend on the considered renormalization scheme.

III. PERTURBATIVE CALCULATION OF 2-POINT CORRELATION FUNCTIONS

We present in this section a strict one-loop calculation (that is, without taking into account RG effects) of gluon and ghost propagators in arbitrary dimension. These correlators require the calculation of four Feynman diagrams as shown in Fig. 1. The corresponding results in $d = 4$ and $d = 3$ are then compared with lattice results, showing a very good agreement (for momenta not much larger than m). Some of these results were presented in [32] but for completeness we review all of them here.

Observing that the gluon propagator is transverse in the Landau gauge, it is convenient to parametrize the gluon $G_{\mu\nu}^{ab}(p)$ and the ghost $G^{ab}(p)$ propagators in the form:

$$G^{ab}(p) = \delta_{ab} F(p)/p^2, \quad G_{\mu\nu}^{ab}(p) = P_{\mu\nu}^{\perp}(p) \delta_{ab} G(p). \quad (7)$$

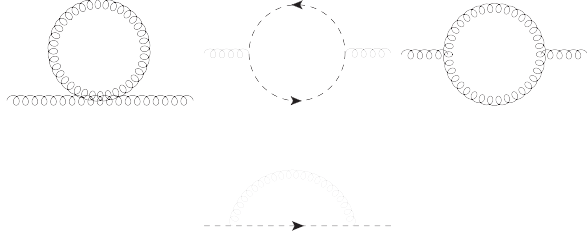


FIG. 1. First line: three diagrams contributing to the gluon self-energy. Second line: diagram contributing to the ghost self-energy.

The $F(p)$ is known as the ghost dressing function and the scalar function $G(p)$ will be referred to as the gluon propagator below. We also define the 2-point vertex functions

$$\Gamma_A^{(2)}(p) = G^{-1}(p), \quad \Gamma_{\bar{c}c}^{(2)}(p) = p^2 F^{-1}(p). \quad (8)$$

We choose the following renormalization conditions for 2-point functions:

$$\begin{aligned} \Gamma_A^{(2)}(p=0) &= m^2, & \Gamma_A^{(2)}(p=\mu) &= m^2 + \mu^2, \\ \Gamma_{\bar{c}c}^{(2)}(p=\mu) &= \mu^2. \end{aligned} \quad (9)$$

We use the Taylor scheme for the coupling [49], defining the coupling constant from the ghost-antighost-gluon vertex when the ghost momentum is zero. Using the fact that this vertex has no quantum corrections, one deduces that (5) is valid also for the finite part of the renormalization factors.

A. Strict perturbative results for 2-point correlation functions

Let us first consider the calculation of the ghost self-energy in arbitrary dimension using dimensional regularization. Only one diagram contributes (see second line of Fig. 1). The only difference with respect to standard Yang-Mills calculations is the form of the bare gluon propagator (2). Introducing Feynman parameters and performing

internal momentum integrals one easily arrives at the following expression for the ghost 2-point vertex:

$$\begin{aligned} \Gamma_{\bar{c}c}^{(2),1\text{ loop}}(p) &= -\frac{g^2 N}{(4\pi)^{d/2}} \frac{p^2}{m^2} \Gamma\left(2 - \frac{d}{2}\right) \\ &\times \int_0^1 dx \left\{ (xm^2 + x(1-x)p^2)^{d/2-2} \right. \\ &\times \left(m^2 + p^2(1-x)^2 + \frac{xm^2 + x(1-x)p^2}{2-d} \right) \\ &\left. - (x(1-x)p^2)^{d/2-2} \left(p^2 x^2 + \frac{x(1-x)p^2}{2-d} \right) \right\}. \end{aligned} \quad (10)$$

The remaining integral can be performed analytically in integer dimensions as discussed below. Let us only mention here the UV divergent part when $d \rightarrow 4$:

$$\Gamma_{\bar{c}c}^{(2),1\text{ loop}}(p) \stackrel{d \rightarrow 4}{\sim} -\frac{3}{2} \frac{g^2 N p^2}{16\pi^2(4-d)}. \quad (11)$$

This is in agreement with previous calculations in the literature [44,51].

Let us now consider the 2-point vertex for gluons. The first diagram contributing to this vertex function is the gluon tadpole (first diagram in the first line of Fig. 1) and gives a contribution:

$$\Gamma_{A,1}^{(2)}(p) = \frac{g^2 N}{(4\pi)^{d/2}} \frac{(d-1)^2}{d} m^{d-2} \Gamma\left(1 - \frac{d}{2}\right). \quad (12)$$

The only effect of this diagram is to renormalize the mass. The second term contributing to the gluon self-energy is the ghost sunset (second diagram in first line of Fig. 1) which reads:

$$\Gamma_{A,2}^{(2)}(p) = \frac{g^2 N}{(4\pi)^{d/2}} p^{d-2} \frac{(\Gamma(\frac{d}{2}))^2 \Gamma(2 - \frac{d}{2})}{(2-d)\Gamma(d)}. \quad (13)$$

Finally, the third diagram contributing to the gluon self-energy is the gluon sunset (third diagram in the first line of Fig. 1). Again, introducing Feynman parameters, we obtain:

$$\begin{aligned} \Gamma_{A,3}^{(2)}(p) &= 2g^2 N \int_0^1 dx \int \frac{d^d q}{(2\pi)^d} \left\{ \frac{2(x^2 p^4 d + (x^2 + 2)q^2 p^2 + q^4)}{m^2 d} \left(\frac{1}{(q^2 + xm^2 + x(1-x)p^2)^2} - \frac{1}{(m^2 + q^2 + x(1-x)p^2)^2} \right) \right. \\ &\left. - \frac{2p^2 + q^2}{(m^2 + q^2 + x(1-x)p^2)^2} + \frac{(d+2)q^6 + (8x^2 - 8x + 2d(x^2 - x + 1) + 5)q^4 p^2 + (d+2)(x^2 - x + 1)^2 q^2 p^4}{d(d+2)m^4} \right. \\ &\left. \times \left(\frac{1}{(m^2(1-x) + q^2 + x(1-x)p^2)^2} - \frac{1}{(m^2 + q^2 + x(1-x)p^2)^2} + \frac{1}{(xm^2 + q^2 + x(1-x)p^2)^2} - \frac{1}{(q^2 + x(1-x)p^2)^2} \right) \right\}. \end{aligned} \quad (14)$$

The integral in the internal momentum q can be done analytically in arbitrary dimensions but the result is lengthy and not particularly illuminating. We can compute the divergent part of the gluon 2-point function, which reads:

$$\Gamma_A^{(2),1\text{ loop}}(p) \stackrel{d \rightarrow 4}{\sim} \frac{g^2 N}{16\pi^2(4-d)} \left(\frac{3}{2} m^2 - \frac{13}{3} p^2 \right). \quad (15)$$

Together with (11), this leads to the determination of the divergent part of the renormalization factors at one loop:

$$Z_{m^2} = 1 - \frac{35}{6} \frac{g^2 N}{16\pi^2} \frac{1}{4-d}, \quad Z_c = 1 + \frac{3}{2} \frac{g^2 N}{16\pi^2} \frac{1}{4-d},$$

$$Z_A = 1 + \frac{13}{3} \frac{g^2 N}{16\pi^2} \frac{1}{4-d}, \quad (16)$$

which coincide with previous results [44,51].

$$G^{-1}(p)/m^2 = s + 1 + \frac{g^2 N s}{384\pi^2} \left\{ 111s^{-1} - 2s^{-2} + (2 - s^2) \log(s) + 2(s^{-1} + 1)^3 (s^2 - 10s + 1) \log(1 + s) \right.$$

$$\left. + (4s^{-1} + 1)^{3/2} (s^2 - 20s + 12) \log\left(\frac{\sqrt{4+s} - \sqrt{s}}{\sqrt{4+s} + \sqrt{s}}\right) - (s \rightarrow \mu^2/m^2) \right\},$$

$$F^{-1}(p) = 1 + \frac{g^2 N}{64\pi^2} \left\{ -s \log(s) + (s + 1)^3 s^{-2} \log(s + 1) - s^{-1} - (s \rightarrow \mu^2/m^2) \right\}, \quad (17)$$

where $s = p^2/m^2$.

In Fig. 2, we compare these expressions for the $SU(2)$ gauge group with the lattice simulations of [25]. The best choice of parameter is $g = 7.5$ and $m = 0.68$ GeV when the normalization prescriptions are imposed at $\mu = 1$ GeV. One observes that both gluon and ghost propagators can be fitted with the same choice of parameters in a very satisfactory way. Note that the normalization conditions used in lattice simulations are not (9). Accordingly, it is necessary to introduce a global multiplicative renormalization factor when comparing the curves.

We have also compared our results with the data of two different lattice studies [28,29] for the $SU(3)$ group. These two data sets have different overall momentum scale and we have rescaled the momenta of the data of [28] for superimposing them with those of [29]. Contrarily to the $SU(2)$ case where data are only available in a small momentum interval up to 1.9 GeV, the data for $SU(3)$ were computed for momenta up to 8 GeV. Consequently one can explore the crossover from standard perturbative results when p is significantly larger than m (requiring RG methods) and an IR regime similar to the one analyzed in the $SU(2)$ case. We represent in Fig. 3 the gluon propagator and the ghost dressing function. We present also the gluon dressing function $p^2 G(p)$ in order to make visible the UV regime. The best choice of parameters is $g = 4.9$ and $m = 0.54$ GeV (again with the renormalization prescription imposed at $\mu = 1$ GeV) and it leads to a very satisfying agreement for momenta $p \lesssim 2$ GeV. Beyond 2 GeV, the agreement is not as good but this is not a surprise because expressions (17) are one-loop results obtained from a fixed coupling constant calculation in a fixed renormalization point. It is well-known that in order to analyze the regime $p \gg m$, one must take into account RG effects and, in

B. Results in $d = 4$

When $d \rightarrow 4$ the expressions for correlation functions (10) and (12)–(14), diverge in the UV. In order to calculate the renormalized 2-point functions, one must consider the sum of those self-energies with a bare contribution with renormalization factors. When d approaches an integer dimension, the remaining integrals can be performed analytically.

Once the renormalization conditions are imposed [see Eq. (9)] the renormalized functions $F(p)$ and $G(p)$ are finite in the limit $d \rightarrow 4$ and read:

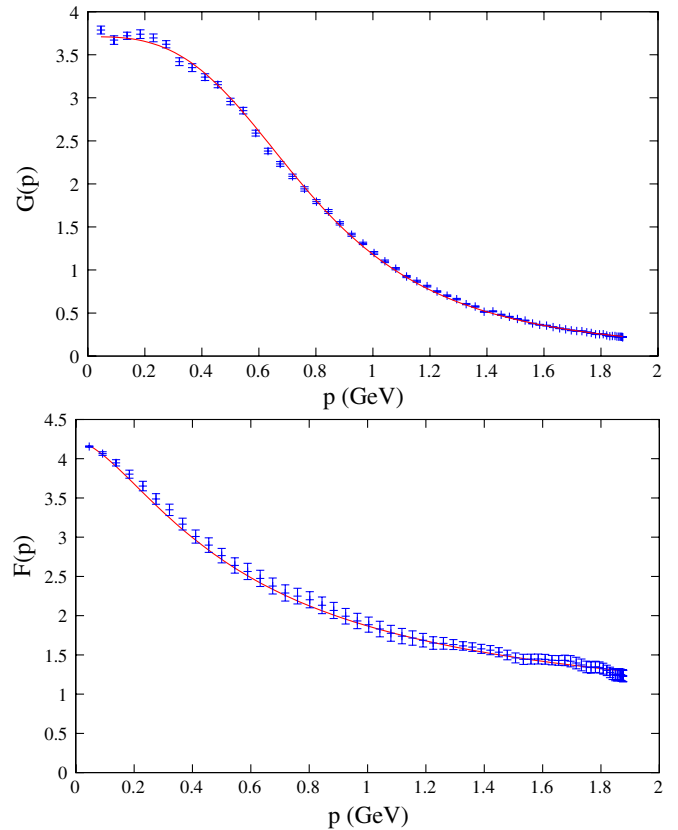


FIG. 2 (color online). Four-dimensional correlation functions for $SU(2)$ gauge group. The results of the present work (red curve) are compared with lattice data of [25] (blue points). Top figure: gluon propagator. Bottom figure: ghost dressing function.

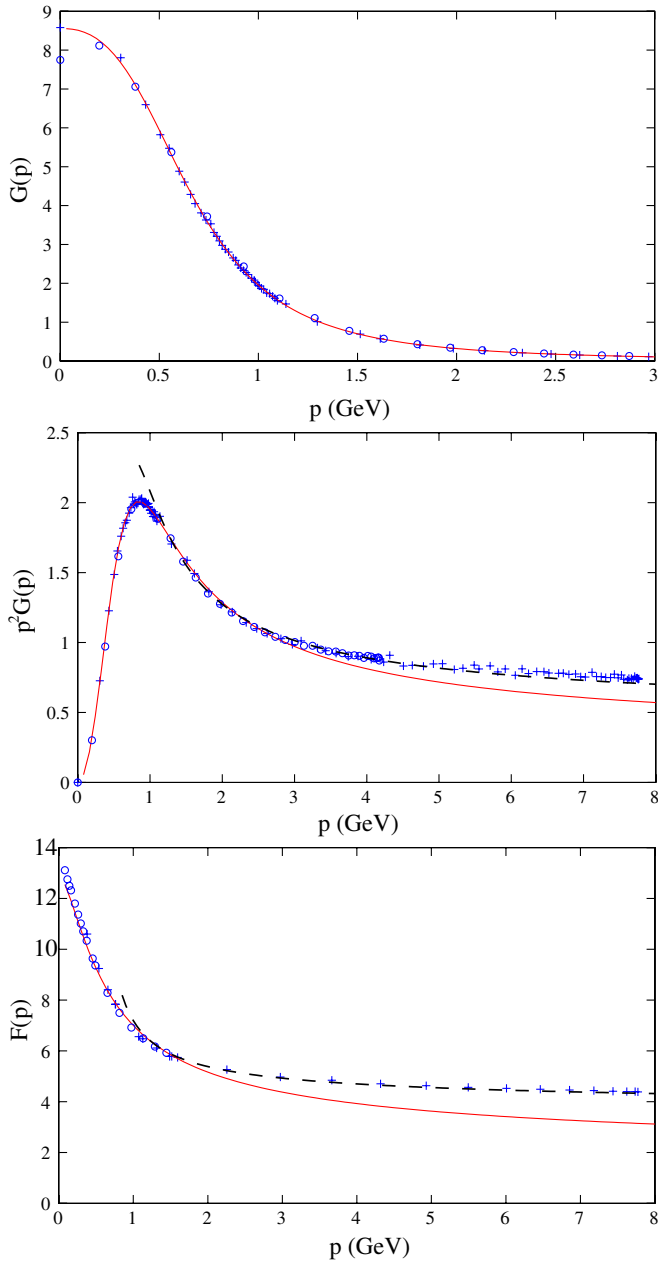


FIG. 3 (color online). Four-dimensional correlation functions for $SU(3)$ gauge group. The results of strict perturbation theory (red solid curve) are compared with lattice data of [28] (blue open circles) and [29] (blue crosses). The black dashed curve is obtained by the zero momentum prescription RG (see Sec. IVA). Top figure: gluon propagator. Middle figure: gluon propagator times p^2 . Bottom figure: ghost dressing function.

particular, the running of the coupling. The corresponding procedure is presented in detail in the next sections. Once RG effects are included, the agreement is essentially within error bars for $p > m$ as is also shown in Fig. 3. In any case, it is obvious that when $p \gg m$, the model (1) reproduces correctly the high momentum regime once RG effects are taken into account because it just coincides in that case with the standard FP model.

A natural question to raise at this point is whether the parameters found by the previous fitting procedure are compatible with other determinations. We choose to compare g with the results of [52] which make use of a very similar renormalization scheme: the coupling is defined through the Taylor scheme and the ghost renormalization factor is fixed by the second line of Eq. (9). The only difference is that the gluon renormalization factor is fixed by the condition $\Gamma_A^{(2)}(p = \mu) = \mu^2$. Because of the non-renormalization theorem of the coupling, this amounts to a relation between the coupling constant $g^{(l)}$ of [52] and ours which reads:

$$g^{(l)} = \frac{g}{\sqrt{1 + \frac{m^2}{\mu^2}}}. \quad (18)$$

We extract from Fig. 1 of Ref. [52] the value $g^{(l)} \simeq 3.5$ at $\mu = 1$ GeV while the right-hand side of (18) leads to 4.3. The error is about 20% which, as discussed below, is the typical estimate of higher loop corrections; see Sec. IVE.

An interesting feature of the one-loop gluon propagator is that it is increasing in the IR. In fact, the inverse propagator behaves at small momenta as $m^2 + Ng^2 p^2 / (192\pi^2) \log(p^2/m^2) + \mathcal{O}(p^2)$. This prediction of our calculation has a very small effect for $d = 4$ and it is not visible in Figs. 2 and 3, but appears clearly in $d = 3$, as shown below.

C. Results in $d = 3$

Let us now consider the three-dimensional case. As in $d = 4$, the 2-point vertex functions can be obtained in an explicit form:

$$\Gamma_{cc}^{(2),1\text{loop}}(p) = \frac{g^2 m N}{32\pi\sqrt{s}} (\pi s^2 + 2\sqrt{s}(1-s) - 2(s+1)^2 \arctan(\sqrt{s})), \quad (19)$$

$$\Gamma_A^{(2),1\text{loop}}(p) = \frac{g^2 m N}{128\pi s^{3/2}} \left(-4(5s^2 + 7s - 1)\sqrt{s} + \pi(s^2 - 2)s^2 - 4(s+1)^2(s^2 - 6s + 1) \times \arctan(\sqrt{s}) + 2s(s+4)(s^2 - 12s + 8) \times \arctan\left(\frac{\sqrt{s}}{2}\right) \right), \quad (20)$$

where again $s = p^2/m^2$.

These expressions are finite because in $d = 4$ all divergences are logarithmic and lowering the dimension reduces the level of UV divergence of any diagram. Accordingly, a possible renormalization scheme could be to use as renormalized parameters just the bare ones (that are finite). However it is well-known that it is more convenient to choose a renormalization scheme where renormalized parameters are defined at a running scale. This corresponds

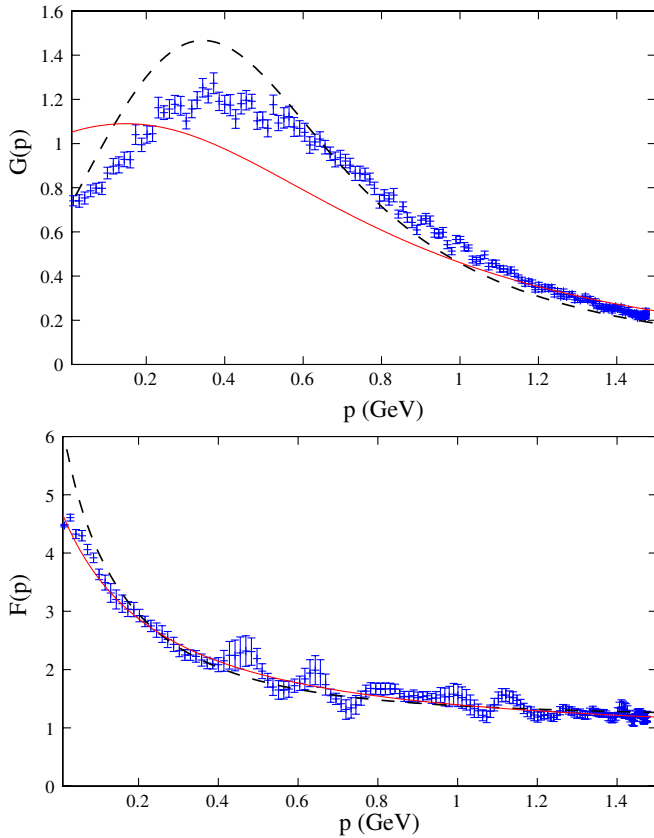


FIG. 4 (color online). Three-dimensional correlation functions for $SU(2)$ gauge group. The results of strict perturbation theory (red solid curve) are compared with lattice data of [25] (blue points). The black dashed curve is the IR safe RG improved result (see Sec. IV B). Top figure: gluon propagator. Bottom figure: ghost dressing function.

to a finite renormalization with respect to the bare parameters. This is convenient in order to avoid large perturbative corrections. Moreover, choosing renormalized parameters at a running scale will allow us to perform a RG analysis in the next sections (that considerably improves the results). In the present section we use the renormalization conditions (9).

The model (1) is able to account for the main features of gluon and ghost propagators found in lattice simulations. In Fig. 4 the results of our calculation with the best fit parameters $g = 3.7\sqrt{\text{GeV}}$ and $m = 0.89 \text{ GeV}$ for $\mu = 1 \text{ GeV}$ are compared with $d = 3$ simulations performed with the gauge group $SU(2)$ [25]. We observe that the best fit for gluon and ghost propagators are not as good as in $d = 4$. We will show below that the inclusion of RG effects improve significantly one-loop results. In any case, our calculation reproduces the finite IR gluon propagator and ghost dressing function. It also reproduces the increasing behavior of the gluon propagator in the IR. Indeed, an expansion of the inverse propagator at low momentum leads to $m^2 - Ng^2p/64 + \mathcal{O}(p^2)$.

IV. RENORMALIZATION GROUP ANALYSIS

We showed in the previous section that the one-loop perturbative results compare very well with the lattice data up to energies of order 2 GeV and get worse at higher energies. This is not a surprise since in $d = 4$ the perturbation theory generates logarithms of the momentum divided by some momentum scale (the mass or the renormalization point μ). The pure perturbation theory fails at energies higher than 2 GeV because these logarithms are large and one needs to implement the ideas of the RG. Actually since we have massless modes (ghosts) in the theory, it is expected *a priori* that the RG analysis is necessary also for $p \ll m$. We will see however that, in this particular model, the IR behavior is milder than expected, essentially because ghosts interact by the exchanging gluons which are massive.

For $d < 4$, the UV behavior does not present large logarithms, and consequently the use of the RG is not mandatory in that regime. However, in practice, taking into account RG effects may improve the quantitative results. This idea is natural, but we are not able to test it because there is no UV data available in $d = 3$ or $d = 2$. For $d < 4$, a RG adapted for the IR is much more important than for $d = 4$ and at the end of the present section we show that such a RG procedure considerably improves the results in $d = 3$. The $d = 2$ case can also be better understood by including the RG effects but the discussion of this point is postponed to Sec. V.

A. Vanishing-momentum prescription scheme in $d = 4$

We recall the main steps of renormalization, mainly to fix the notations. We concentrate in this section on the renormalization prescriptions that were described in Sec. II. We define the β functions and anomalous dimensions as:

$$\beta_g(g, m^2) = \mu \left. \frac{dg}{d\mu} \right|_{g_B, m_B^2}, \quad (21)$$

$$\beta_{m^2}(g, m^2) = \mu \left. \frac{dm^2}{d\mu} \right|_{g_B, m_B^2}, \quad (22)$$

$$\gamma_A(g, m^2) = \mu \left. \frac{d \log Z_A}{d\mu} \right|_{g_B, m_B^2}, \quad (23)$$

$$\gamma_c(g, m^2) = \mu \left. \frac{d \log Z_c}{d\mu} \right|_{g_B, m_B^2}. \quad (24)$$

We can then use the RG equation:

$$\left(\mu \partial_\mu - \frac{1}{2} (n_A \gamma_A + n_c \gamma_c) + \beta_g \partial_g + \beta_{m^2} \partial_{m^2} \right) \Gamma^{(n_A, n_c)} = 0, \quad (25)$$

to relate the 2-point vertex functions at different scales:

$$\Gamma_A^{(2)}(p, \mu, g(\mu), m^2(\mu)) = z_A(\mu)\Gamma_{AA}^{(2)}(p, \mu_0, g(\mu_0), m^2(\mu_0)), \quad (26)$$

$$\Gamma_{\tilde{c}c}^{(2)}(p, \mu, g(\mu), m^2(\mu)) = z_c(\mu)\Gamma_{\tilde{c}c}^{(2)}(p, \mu_0, g(\mu_0), m^2(\mu_0)), \quad (27)$$

where $g(\mu)$ and $m^2(\mu)$ are obtained by integration of the beta functions with initial conditions given at some scale μ_0 and:

$$\begin{aligned} \log z_A(\mu) &= \int_{\mu_0}^{\mu} \frac{d\mu'}{\mu'} \gamma_A(g(\mu'), m^2(\mu')), \\ \log z_c(\mu) &= \int_{\mu_0}^{\mu} \frac{d\mu'}{\mu'} \gamma_c(g(\mu'), m^2(\mu')). \end{aligned} \quad (28)$$

Using the normalization conditions described in Sec. II, we then get:

$$\Gamma_A^{(2)}(p, \mu_0, g, m^2) = \frac{p^2 + m^2(p)}{z_A(p)}, \quad (29)$$

$$\Gamma_{\tilde{c}c}^{(2)}(p, \mu_0, g, m^2) = \frac{p^2}{z_c(p)}. \quad (30)$$

The renormalization scheme considered here leads to a relation between the β functions and the anomalous dimensions γ_A and γ_c . As explained before, in the Taylor scheme the nonrenormalization theorem (5) is also valid for the finite parts. This leads to the following expression for the β function of the coupling constant:

$$\beta_g(g, m^2) = g \left(\frac{\gamma_A(g, m^2)}{2} + \gamma_c(g, m^2) \right). \quad (31)$$

The choice of a normalization prescription at vanishing momentum for the gluon 2-point vertex simplifies greatly the analytical treatment because as shown in Appendix A the following relation is satisfied for the finite parts of the propagators and dressing functions:

$$\Gamma_A^{(2)}(p=0) = Z_A m_B^2 F_B(p=0). \quad (32)$$

It is then easy to prove that:

$$\beta_{m^2}(g, m^2) = m^2 \gamma_A(g, m^2). \quad (33)$$

The perturbative results together with the renormalization scheme (9) enable us to compute the anomalous dimensions. We get:

$$\begin{aligned} \gamma_A &= -\frac{g^2 N}{192\pi^2 t^3} \left(t(34t^2 - 175t + 6) - 2t^5 \log t \right. \\ &\quad + 2(t+1)^2(2t^3 - 11t^2 + 20t - 3) \log(t+1) \\ &\quad + 2t^{3/2} \sqrt{t+4}(t^3 - 9t^2 + 20t - 36) \\ &\quad \left. \times \log \left(\frac{\sqrt{t+4} - \sqrt{t}}{\sqrt{t+4} + \sqrt{t}} \right) \right), \end{aligned} \quad (34)$$

$$\begin{aligned} \gamma_c &= -\frac{g^2 N}{32\pi^2 t^2} (2(t+1)t - t^3 \log t \\ &\quad + (t+1)^2(t-2) \log(t+1)), \end{aligned} \quad (35)$$

where $t = \mu^2/m^2$.

These expressions for the anomalous dimensions lead, together with Eqs. (31) and (33), to the expressions of the β functions. Observe that these β functions are not only functions of the coupling constant g (as, for example, if we use the $\overline{\text{MS}}$ scheme), but also depend on the dimensionless ratio μ^2/m^2 . In principle, once these flow equations are integrated with some appropriate initial conditions, we would need to make another integral to determine $z_A(\mu)$ and $z_c(\mu)$ [see Eq. (28)] in order to determine the inverse propagators. However, since the flows of g and m^2 are expressed in terms of the anomalous dimensions for the ghost and gluon fields, these integrals can be done explicitly:

$$z_A(\mu) = \frac{m^2(\mu)}{m^2(\mu_0)}, \quad (36)$$

$$z_c(\mu) = \frac{g(\mu)}{g(\mu_0)} \sqrt{\frac{m^2(\mu_0)}{m^2(\mu)}}. \quad (37)$$

Studying the behavior of these anomalous dimensions for μ much larger and much smaller than m together with Eq. (31), we find:

$$\beta_g \sim \begin{cases} -\frac{g^3 N}{16\pi^2} \frac{11}{3} & \text{if } \mu \gg m, \\ -\frac{g^3 N}{16\pi^2} \frac{1}{12} & \text{if } \mu \ll m. \end{cases} \quad (38)$$

In the UV ($\mu \gg m$) we obtain the standard, universal, β function. This is in contrast to other approaches where masses are introduced in Yang-Mills theory but modifying the UV behavior of the model [41]. In the IR ($\mu \ll m$), we observe that, although smaller in absolute value than in the UV, β_g remains negative which means that the coupling constant diverges at a finite energy scale: we encounter a Landau pole in the integration.

However, we stress that there are no large quantum corrections when $p \ll m$ (at least when $d > 2$) because there are no IR divergences. In this configuration, a natural scheme is to use strict perturbation theory for $p \lesssim m$ and a RG improvement when $p \gtrsim m$. The absence of IR divergences might be surprising since the ghosts are massless. A simple way of understanding this is to observe that all diagrams, except those with a single ghost loop, include at least one gluon propagator, which regularize the IR behavior (this issue is discussed in more detail in Appendix B). In this sense a purely perturbative calculation for momenta $p \lesssim 1$ GeV and a RG improvement for UV regime ($p \gtrsim 1$ GeV) is fully justified. In practice, since the RG flow presents a Landau pole at an energy scale not far from 1 GeV, we want to make the matching

at a higher energy, but lower than 2 GeV, where strict perturbation theory begins to become untrustworthy. A compromise is to perform the matching condition at 1.5 GeV and this gives impressively good results, as can be seen in Fig. 3.

B. IR safe scheme in $d = 4$

A drawback of the procedure described in the previous section is that there is some arbitrariness in the choice of the matching scale to join strict perturbative and RG results. In this sense a unified procedure, valid at all scales, would be more satisfactory and this motivates the search for an IR safe RG scheme.

In this respect, it is interesting to note that the IR Landau pole that appears in the previous RG scheme is not a physical effect but is actually a consequence of our renormalization scheme (9). Indeed, the prescriptions we chose there are *not* consistent, if μ is too small, with the one-loop results (and with the actual behavior observed in lattice simulations in $d = 3$) that lead to an increasing propagator in the IR (see Sec. III). In order to avoid this problem and be able to take renormalization prescriptions at arbitrary scales, we present here a scheme which is not based on an explicit constraint of the 2-point vertex function but which comes from the nonrenormalization theorem (6). In practice, we replace the first condition in (9) by imposing the relation:

$$Z_A Z_c Z_{m^2} = 1, \quad (39)$$

not only for the divergent parts but also for the finite parts. The renormalized mass m^2 does not correspond any more to the value of the renormalized propagator at zero momentum and accordingly there is no contradiction with the increase of the propagator in the IR.

Within this new scheme, few formulas must be modified. The β function for the mass is now changed to:

$$\beta_{m^2}(g, m^2) = m^2(\gamma_A(g, m^2) + \gamma_c(g, m^2)). \quad (40)$$

The anomalous dimension for the ghost is unchanged [see Eq. (35)] while the anomalous dimension for the gluon field reads:

$$\begin{aligned} \gamma_A = & \frac{g^2 N}{96\pi^2 t^3} \left(-(t-2)^2(2t-3)(t+1)^2 \log(t+1) \right. \\ & + (-17t^2 + 74t - 12)t + t^5 \log(t) \\ & \left. - t^{3/2} \sqrt{t+4}(t^3 - 9t^2 + 20t - 36) \log\left(\frac{\sqrt{t+4} - \sqrt{t}}{\sqrt{t+4} + \sqrt{t}}\right) \right), \end{aligned} \quad (41)$$

where, as before, $t = \mu^2/m^2$. Finally, the expressions relating $z_A(\mu)$ and $z_c(\mu)$ to the coupling constants read now:

$$z_A(\mu) = \frac{m^4(\mu)}{m^4(\mu_0)} \frac{g^2(\mu_0)}{g^2(\mu)}, \quad (42)$$

$$z_c(\mu) = \frac{g^2(\mu)}{g^2(\mu_0)} \frac{m^2(\mu_0)}{m^2(\mu)}. \quad (43)$$

The UV universal behavior of the β function (for $\mu \gg m$) is unchanged as expected. However, we observe that the beta function for the coupling constant in the IR is now *positive*:

$$\beta_g \sim \frac{g^3 N}{16\pi^2} \frac{1}{6} \quad \text{if } \mu \ll m. \quad (44)$$

We need to insist on the fact that the universality of the beta function is only valid for mass-independent schemes or for $\mu \gg m$ up to two-loop order. In particular, for $\mu \lesssim m$ there is no reason for the beta function to be scheme-independent and it is typically not the case. The result (44) means that in the present scheme, the IR behavior is possibly safe. Actually, depending on the initial conditions of the flow we do, or do not, hit a Landau pole. (Obviously, if we start with a vanishing mass, we retrieve the standard one-loop calculation and we do hit the Landau pole, so a sufficiently large initial mass is necessary to be IR safe).

A second consequence of this IR behavior is that if the flow does not hit a Landau pole, then the coupling constant is attracted towards zero in the IR: the massive Gaussian fixed point is attractive. This is a very appealing property because this justifies the use of perturbation theory in the regime $p \ll m$, although its use at intermediate momenta ($p \sim m$) is more delicate. The validity of perturbation theory at intermediate momenta is discussed in Sec. IV E.

In Fig. 5 the results for the correlation functions obtained from the numerical integration of the RG equations for the coupling and mass are presented. The best choice of parameters at the scale $\mu = 1$ GeV is $g = 3.7$ and $m = 0.39$ GeV. One observes a very good agreement of the one-loop RG result when compared with lattice simulations, particularly, as expected, in the UV and in the IR. The only region where a significative departure is seen is for intermediate momenta ($1 \text{ GeV} \lesssim p \lesssim 2 \text{ GeV}$) for the gluon dressing function. The results, however, are not as good as those obtained with the scheme of Sec. IV A. This may be surprising and we now explain why it is not so. First, as already mentioned and explained in detail in Appendix B, there are no IR divergences and consequently the use of RG analysis is not mandatory for $p \lesssim m$. Second, the results of the previous section have been obtained by a mixed treatment, by using the best fit of strict perturbation theory and imposing a matching with RG results in the UV. The results discussed here are obtained with a unified treatment, valid at all scales. This is a more challenging situation because we do not have the freedom of choosing the matching scale. In this sense the IR safe scheme gives a more satisfying construction. Third, as discussed in

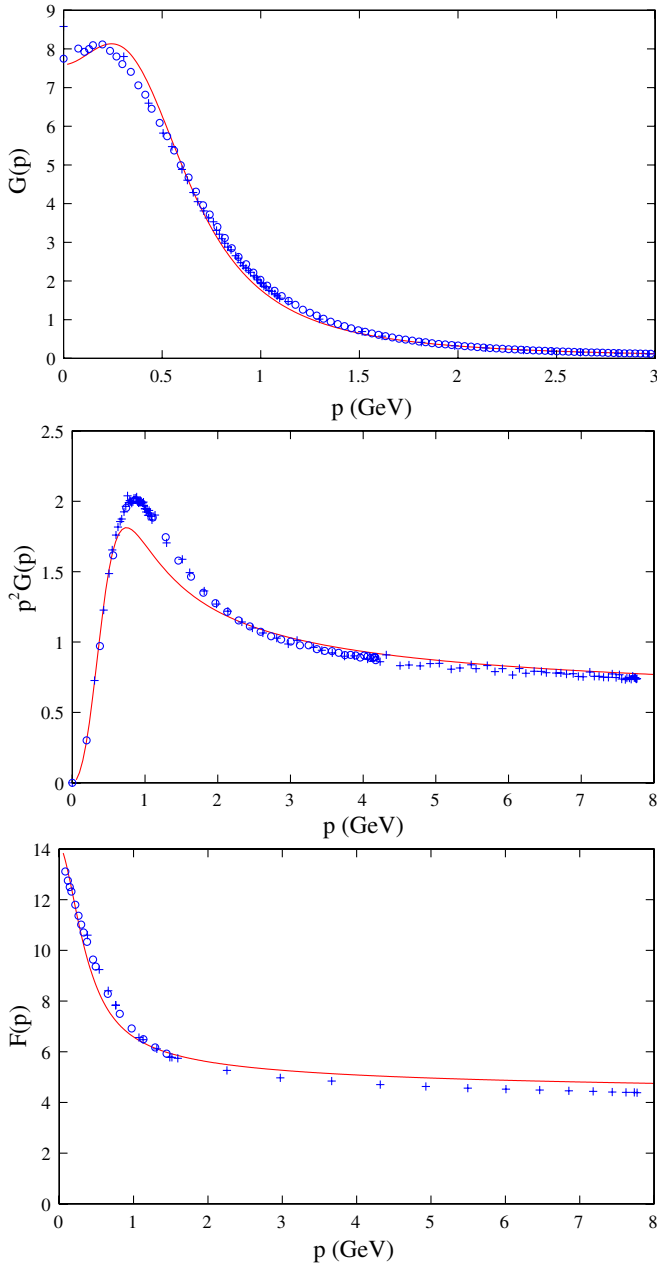


FIG. 5 (color online). Four-dimensional correlation functions for the $SU(3)$ gauge group. The results obtained by the IR safe RG (see Sec. IV B) (red solid line) are compared with lattice data of [28] (blue open circles) and [29] (blue crosses). Top figure: gluon propagator. Middle figure: gluon propagator times p^2 . Bottom figure: ghost dressing function.

Sec. IV E, even if the relevant coupling in the present model is never large, it is nevertheless not very small. Accordingly the results obtained in the present section are quite satisfactory and the surprise is more the level of precision achieved in the previous one. A possible explanation is that the choice of RG prescriptions that can be directly read from correlation functions [and not from an implicit RG scheme as done in (39)], may in practice reduce the contributions of higher loop corrections. In

any case we may expect that two-loop corrections should improve considerably the present results and correspondingly reduce the scheme dependence of them. Finally, the coupling constant compares much better with the one extracted from lattice simulations [see Eq. (18)]. Taking into account the difference of renormalization scheme, we now find, at $\mu = 1$ GeV, $g^{(l)} = 3.4$ which compares very well with the lattice data 3.5 [52]; see Eq. (18).

C. The IR behavior in arbitrary dimensions

Before discussing the results in $d = 3$, it is convenient to study the IR ($\mu \ll m$) behavior of RG functions of the model in arbitrary dimensions. We saw in the previous subsection that, in that regime, the beta function for the coupling constant is positive and accordingly the Gaussian IR fixed point is attractive. When $d \neq 4$, the coupling constant g has dimension $[\text{energy}]^{(4-d)/2}$ and it is convenient to introduce the dimensionless coupling

$$\tilde{g}(\mu) = g(\mu)\mu^{(d-4)/2}, \quad (45)$$

in order to analyze a process with characteristic momentum μ . Of course, it may be appropriate to use powers of the mass in order to define a dimensionless coupling. This point is discussed below (see Sec. IV E), but for the moment let us concentrate on the choice (45) which is the natural definition of the dimensionless coupling in the UV regime ($\mu \gg m$). The β function associated with \tilde{g} is:

$$\beta_{\tilde{g}} = \mu \frac{\partial(g\mu^{(d-4)/2})}{\partial\mu} = -\frac{4-d}{2}\tilde{g} + \mu^{(d-4)/2}\beta_g. \quad (46)$$

For dimensional reasons, the function $\beta_{\tilde{g}}$ is only a function of \tilde{g} and of the dimensionless squared mass:

$$\tilde{m}^2 = m^2\mu^{-2}. \quad (47)$$

For any $d < 4$, as well known, in the UV regime ($\mu \gg m$ or, equivalently $\tilde{m}^2 \ll 1$), the coupling \tilde{g} approaches rapidly a Gaussian fixed point because of the dominance of the dimensional term $-\frac{4-d}{2}\tilde{g}$. The case $d = 4$ is also dominated by a Gaussian fixed point in the UV, because of the negative sign of the g^3 term. At intermediate momenta $\mu \sim m$, the expressions of the $\beta_{\tilde{g}}$ function are very complicated in arbitrary dimensions and its (nonilluminating) expression involves special functions. However in the IR regime $\mu \ll m$ things become easier again, and one can give an explicit expression for the $\beta_{\tilde{g}}$ function at one-loop:

$$\beta_{\tilde{g}} = -\frac{4-d}{2}\tilde{g} + \frac{(4-d)(d-2)\pi^{(3-d)/2}}{2^{2d+1}\Gamma(\frac{d+1}{2})\sin(\frac{(4-d)\pi}{2})}N\tilde{g}^3. \quad (48)$$

The coefficient of the \tilde{g}^3 term is regular (and nonzero) in all dimensions $d > 0$. One observes the appearance of an IR fixed point \tilde{g} :

$$N\tilde{g}_*^2 = \frac{4^d \Gamma(\frac{d+1}{2}) \sin(\frac{(4-d)\pi}{2})}{(d-2)\pi^{(3-d)/2}}. \quad (49)$$

When $d \rightarrow 4$, expression (48) approaches the $d = 4$ result (44) and the fixed point value approaches the Gaussian limit $\tilde{g}_*^2 = 0$.

The coherence of these results relies on the hypothesis that $\tilde{m}^2 \rightarrow \infty$, when $\mu \rightarrow 0$. To check this hypothesis, we write the β function for the dimensionless mass \tilde{m}^2 :

$$\beta_{\tilde{m}^2} = \mu \frac{\partial(m^2 \mu^{-2})}{\partial \mu} = -2\tilde{m}^2 + \mu^{-2} \beta_{m^2}. \quad (50)$$

As before, the UV regime (where $\tilde{g} \rightarrow 0$) is compatible with $\tilde{m}^2 \rightarrow 0$ and this can already be seen in the $\sim -2\tilde{m}^2$ term. The intermediate momentum regime ($\mu \sim m$) gives complicated expressions, but the IR regime again simplifies to:

$$\beta_{\tilde{m}^2} = -2\tilde{m}^2 + N\tilde{g}^2 \tilde{m}^2 \frac{(4-d)(d-2)\pi^{(3-d)/2}}{4^d \Gamma(\frac{d+1}{2}) \sin(\frac{(4-d)\pi}{2})}. \quad (51)$$

Note that the prefactor of $\tilde{g}^2 \tilde{m}^2$ of this expression is twice the prefactor of \tilde{g}^3 in Eq. (48). Consequently when \tilde{g}^2 approaches its IR fixed point:

$$\beta_{\tilde{m}^2} \sim (2-d)\tilde{m}^2. \quad (52)$$

For $d > 2$, this implies that a regime with $\tilde{m}^2 \rightarrow \infty$ and $\tilde{g} \sim \tilde{g}_*$ exists (under the hypothesis that the flow does not hit a Landau pole before approaching it). Note that the dimensionless square mass diverges as μ^{2-d} , but the dimensionful mass goes to zero for $d < 4$. This is not incompatible with the fact the gluon propagator is finite in the zero momentum limit, because in the present scheme, the mass is *not* defined through the renormalization condition (9). It is easy to show that:

$$\lim_{p \rightarrow 0} \Gamma_A^{(2)}(p) = \frac{\tilde{g}_*^2 m^4(\mu_0)}{\tilde{m}_{\text{as}}^2 g^2(\mu_0)}, \quad (53)$$

where $\tilde{m}^2(p) \sim \tilde{m}_{\text{as}}^2 p^{2-d}$. The $d = 2$ case is different. In that dimension, the coupling constant would approach a fixed point in an hypothetical IR regime, but the leading contribution to the flow of \tilde{m}^2 is zero and one must analyze subleading contributions. This important particular case is analyzed in Sec. V.

D. IR safe scheme in $d = 3$

Having considered the general IR behavior, we now repeat the calculation of the Sec. IV B in the $d = 3$ case and compare the results with the lattice simulations. The calculation now leads to the following anomalous dimensions:

$$\begin{aligned} \gamma_A = & \frac{g^2 N}{128 \mu \pi t^2} (\pi t^2 (-3t^2 + 2) + 4\sqrt{t}(7t^2 - 29t + 15) \\ & - 2t(3t^3 - 8t^2 + 40t - 96) \arctan(\sqrt{t}/2) \\ & + 4(3t^4 - 4t^3 + 8t^2 - 15) \arctan(\sqrt{t})), \end{aligned} \quad (54)$$

$$\begin{aligned} \gamma_c = & \frac{g^2 N}{32 \mu \pi t} (-\pi t^2 + 2\sqrt{t}(t + 3) \\ & + 2(t + 1)(t - 3) \arctan(\sqrt{t})), \end{aligned} \quad (55)$$

where again $t = \mu^2/m^2$. We then deduce the β functions for g and m^2 via the nonrenormalization theorems (31) and (40). For some initial conditions the flow shows a Landau pole, but for the particular values of couplings that do match with numerical simulations, there is no Landau pole. The dimensionless running mass $\tilde{m}(\mu)$ increases when μ decreases and we get an IR regime when $\mu \ll m$. As discussed in the previous section, this regime is characterized by the $\mu \ll m$ limit of the function $\beta_{\tilde{g}}$ that for $d = 3$ is

$$\beta_{\tilde{g}} \sim -\frac{\tilde{g}}{2} + \frac{N\tilde{g}^3}{128}, \quad (56)$$

and the corresponding IR fixed point is

$$N\tilde{g}_*^2 = 64. \quad (57)$$

In the Sec. IV E it is discussed why, in fact, these couplings are not as large as it seems here. We want here only to discuss the corresponding consequences for gluon and ghosts propagators. The RG equations can be integrated numerically and from them the propagators can be obtained as discussed in the $d = 4$. The corresponding results are presented in Fig. 4. We note that the inclusion of these RG running considerably improve the results when compared with those of strict one-loop perturbative results and now compare very well with lattice simulations. This is not surprising, because even if the present model does not have IR divergences it is very common that RG effects play an important role in field theories below four dimensions even at moderate values of the couplings.

E. An estimate of higher loop corrections

The coupling constants that appear throughout this work are frequently relatively large at intermediate scales $\mu \sim 1$ GeV. This situation is much better than having a Landau pole, but it is problematic for a perturbative analysis. In this section we argue that although the coupling constant is not small, the perturbation theory seems to be under control anyway.

First of all, as is well known [53], the parameter expansion is not g^2 but, because of angular factors and group factors:

$$u(p) = \frac{g^2(p)Np^{d-4}}{(4\pi)^{d/2}\Gamma(d/2)}, \quad (58)$$

where p is the momentum scale used to define the coupling constant. In $d \neq 4$, g has dimension $p^{(4-d)/2}$ and the power of momenta in the previous formula is necessary in order to have a dimensionless expansion parameter. The angular factors considerably reduce the size of the expansion parameter. For example, for $d = 4$ and $N = 3$, this expansion parameter has a maximum at values of order one as shown in Fig. 6.

There is actually another effect that suppresses the radiative corrections in the IR as we discuss now in detail. Note that when momenta are much smaller than the gluon mass, all diagrams that include internal gluon lines are suppressed by inverse powers of the gluon mass. This has two consequences. First, as shown in Appendix B, the present model does not present IR divergences for $d > 2$ at nonexceptional momenta. This is surprising at first sight since there are massless modes (ghosts), but it can be understood because their interactions are mediated by massive gluons. A second consequence is that in that regime, the leading contributions are those with a minimum number of gluon propagators and we can consider an effective theory where the only dynamical degrees of freedom are the (massless) ghosts. In this effective theory, gluons appear only as external sources coupled to the ghosts via the bare ghost-gluon vertex while the ghosts interact via an effective 4-point vertex that behaves as $p_1 p_2 g^2/m^2$, where p_1 and p_2 are the antighost momenta [54]. This implies that the effective expansion parameter is suppressed by p^2/m^2 , where p is a typical external momentum. A naive interpolation between the UV parameter expansion u given in (58) and the one relevant for the IR would be:

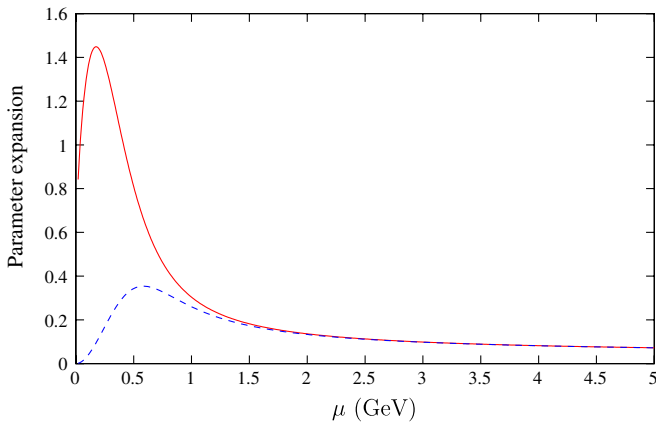


FIG. 6 (color online). Four-dimensional expansion parameter for $SU(3)$. Solid curve (red), $u(\mu)$ is the dimensionless parameter expansion, valid in the UV. Dashed curve (blue), $u(\mu)\mu^2/(\mu^2 + m^2(\mu))$ takes into account the IR freeze-out. The parameters are fixed at 1 GeV as in Sec. IV B.

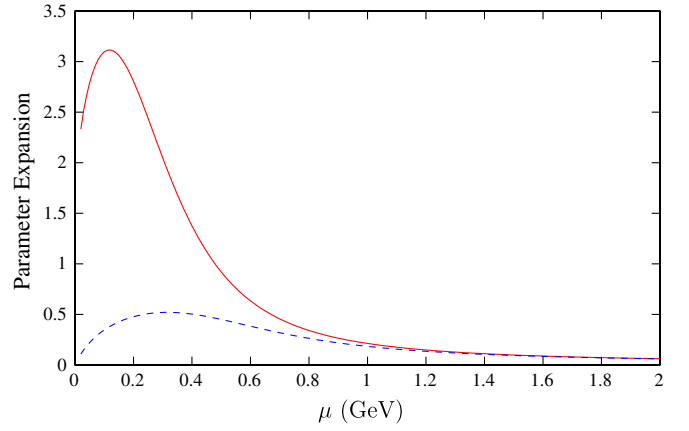


FIG. 7 (color online). Three-dimensional expansion parameter for $SU(2)$. Solid curve (red), $u(\mu)$ is the dimensionless parameter expansion, valid in the UV. Dashed curve (blue), $u(\mu)\mu^2/(\mu^2 + m^2(\mu))$ takes into account the IR freeze-out. The parameters are fixed as in Sec. IV D.

$$u(p) \frac{p^2}{p^2 + m^2} = \frac{g^2(p)Np^{d-2}}{(4\pi)^{d/2}\Gamma(d/2)(m^2 + p^2)}. \quad (59)$$

As shown in Fig. 6 this parameter is indeed relatively small and this makes a perturbative analysis well founded. Actually, in a small region around 1 GeV, the expansion parameter is of the order of 0.4. This means that two-loop corrections in this region will give contributions of order 0.4^2 ($\sim 15\%$), which fits with the discrepancy between the one-loop results and the lattice results shown in Fig. 5. A two-loop calculation would give a more precise estimate of higher order corrections.

Similar results apply for other values of N and d . As an example, the same curve is presented for $N = 2$ and $d = 3$ in Fig. 7. It is shown that the actual values in the IR are slightly larger but remain relatively small.

V. DISCUSSION OF THE $d = 2$ CASE

The explicit expression for propagators can also be obtained in $d = 2$. As before, there are no UV divergences for the same reasons as for $d = 3$. The corresponding result is:

$$\Gamma_{\tilde{c}\tilde{c}}^{(2),1\text{ loop}}(p) = \frac{g^2 N}{8\pi} (s \log(s) - (s+1) \log(s+1)), \quad (60)$$

$$\Gamma_A^{(2),1\text{ loop}}(p) = \frac{g^2 N}{16\pi s} \left(-2(s-1)^2(s+1) \log(s+1) - \sqrt{s(s+4)} \log\left(\frac{\sqrt{s+4} - \sqrt{s}}{\sqrt{s+4} + \sqrt{s}}\right) (s-2)^2 + s(s^2 - 2) \log(s) \right), \quad (61)$$

where, again $s = p^2/m^2$.

Within the model, the difference between $d = 2$ and $d > 2$ which is observed in the lattice (see the introduction) appears natural. In $d = 2$, we find that the gluon propagator and ghost dressing function develop logarithmic divergences when $p \rightarrow 0$:

$$G^{-1}(p) \sim -\frac{g^2 N}{4\pi} \log\left(\frac{p}{m}\right), \quad F^{-1}(p) \sim \frac{g^2 N}{4\pi m^2} \log\left(\frac{p}{m}\right). \quad (62)$$

Such divergences exclude the possibility of controlling a strict one-loop calculation as was used above for $d > 2$. A proper treatment of the $d = 2$ case requires a RG approach adapted to the IR regime.

As shown in Appendix B, the IR convergence of the loop integrals in $d = 2$ does not improve when increasing the order of perturbation theory, as it does for $d > 2$. This is the typical situation at the upper critical dimension of a model and it is well-known that a RG treatment is then necessary to study the IR behavior. We therefore apply the IR safe scheme described in Sec. IV B in the $d = 2$ case.

The anomalous dimensions read:

$$\gamma_A = \frac{g^2 N}{8\pi\mu^2 t} \left(-t^3 \log(t) + 2(t^3 - 4) \log(1 + t) + \sqrt{\frac{t}{4+t}} (t-2)(t^2 + 4t + 12) \log\left(\frac{\sqrt{t+4} - \sqrt{t}}{\sqrt{t+4} + \sqrt{t}}\right) \right), \quad (63)$$

$$\gamma_c = -\frac{Ng^2}{4\pi\mu^2} \log(1 + t), \quad (64)$$

with $t = \mu^2/m^2$. As before, we can extract from them the β functions for the mass and coupling constant. As discussed at the end of Sec. IV C, the leading behavior of the flow of the dimensionless mass is vanishing in $d = 2$. In order to study the IR behavior, it is convenient to consider the following dimensionless combination:

$$\lambda = \frac{g}{m}, \quad (65)$$

whose β function takes the form:

$$\beta_\lambda = \frac{\lambda}{2} \gamma_c = -\frac{N\lambda^3}{8\pi} \frac{\log(1+t)}{t}.$$

Observe that this β function is always negative and therefore leads to a IR Landau pole. The only way round would be that $\tilde{m}^2 = 1/t$ would run to zero sufficiently fast when μ decreases. However the study of the flow of \tilde{m}^2 in the IR is at odds with this hypothesis. Indeed, the β function for \tilde{m}^2 behaves at small \tilde{m}^2 as:

$$\beta_{\tilde{m}^2} = -\tilde{m}^2 \left(2 + \frac{N\lambda^2}{\pi} \frac{\log(t)}{t} \right), \quad (66)$$

which leads to an increase of \tilde{m}^2 in the IR.

In conclusion, the case $d = 2$ is very different from higher dimensions: There is no fixed point and the flow runs to a Landau pole. We relate this first property with the observation that, in $d = 2$ and for $\mu \ll \tilde{m}^2$, the β functions for g and \tilde{m}^2 are proportional [see Eqs. (48) and (51)]:

$$2 \frac{\beta_{\tilde{g}}}{\tilde{g}} = \frac{\beta_{\tilde{m}^2}}{\tilde{m}^2}. \quad (67)$$

A similar situation appears in the random mass Ising model [55] which is characterized by two ϕ^4 coupling constants. The associated β functions are found to be proportional (in the sense of the previous equation) at leading order in the ϵ expansion. The two-loop calculation [56,57] lifts this degeneracy and yields a fixed point with coupling constants $\sim \sqrt{\epsilon}$. It would be interesting to study if the two-loop contributions lift in the same manner the degeneracy of the β functions for \tilde{g} and \tilde{m}^2 .

VI. CONCLUSION

We have shown in detail that a particular case of the Curci-Ferrari model, motivated by phenomenological considerations reproduces quantitatively several nontrivial correlation functions of pure gluodynamics in all ranges of momenta. The result is obtained from a very simple one-loop perturbative calculation and the surprising agreement is justified by estimating the size of higher loop corrections. Moreover, we have proposed an IR safe RG scheme that does not show a Landau pole. Therefore we have at hand a phenomenological model that correctly describes Yang-Mills correlators. These results question the common idea that the IR properties of QCD are beyond the scope of perturbation theory.

At the conceptual level, it would be more satisfying to be able to calculate the mass parameter from first principles and this is probably a nonperturbative and very difficult issue (see however [36,37]). However, once the existence of this mass is accepted, the rest of the analysis seems to be purely perturbative. The determination of the mass from first principles would be also interesting since it would fix the results in terms of the single parameter appearing in pure Yang-Mills theory. Another important open issue is that of the unitarity of the model. As discussed in Sec. II, the usual proofs of unitarity do not work in this model because the nilpotency of the BRST symmetry is broken. The situation is actually common to all schemes beyond the FP procedure, such as the GZ model, but it does not unavoidably mean that the model breaks unitarity. It could be that a procedure permits one to reduce the state space down to a physical Hilbert space (where unitarity is recovered) that would not rely on the nilpotency of the BRST operator. Devising such a procedure is an open issue.

Beyond these fundamental problems, the evidences that the model considered here is a good and simple phenomenological one opens the way to many applications. Let us mention here some of them. The 3-point correlation

functions have been measured on the lattice and their calculation is a direct extension of the work presented here and would give another test of the ability of the model to reproduce Yang-Mills correlation functions. It would also be interesting to compute the two-loop contributions to the ghost and gluon propagators, that would, in particular, give a direct measure of the size of higher order corrections. The calculation of RG flows and 2-point correlation functions can be easily extended at finite temperature and many thermodynamic properties can be extracted from it. Of great physical interest would be to calculate within this model the quark-antiquark potential in the quenched approximation, although it is hard to believe that confinement would appear in such a simple analysis. Let us mention finally that introducing matter fields is straightforward and studying the influence of the quarks on the ghost and gluon correlation functions is a natural extension of this work.

ACKNOWLEDGMENTS

We thank A. Cucchieri, O. Oliveira, M. Mueller-Preussker, and A. Sternbeck for useful correspondence. M. T. thanks the IFFI for its hospitality. N. W. acknowledges the support of the PEDECIBA program.

APPENDIX A: NONRENORMALIZATION THEOREM FOR THE MASS

We derive in this appendix the nonrenormalization theorem for the mass. We used this result in Sec. IV A to simplify the RG analysis. The main part of the proof is done with bare quantities but in order to simplify the notations we omit the subscript B .

The proof makes use of the Slavnov-Taylor identity and we therefore introduce sources not only for the primary fields A_μ , c , \bar{c} , and h , but also for their BRST variations. The partition function then reads:

$$e^W = \int \mathcal{D}A_\mu \mathcal{D}c \mathcal{D}\bar{c} \mathcal{D}h e^{-S+S_{\text{sources}}}, \quad (\text{A1})$$

where

$$S_{\text{sources}} = \int d^d x (J_\mu A_\mu + \bar{\chi} c + \bar{c} \chi + Rh + \bar{K} s A_\mu + \bar{L} s c), \quad (\text{A2})$$

and S is the integral of the Lagrangian (1). The BRST variations s of the fields are defined as the prefactors of η in the right-hand sides of (3). It is not necessary to introduce sources for the variation of h or for the variations of the primary fields since these are either vanishing or linear in the primary fields. We also introduce the Legendre transform as:

$$\Gamma + W = \int d^d x (J_\mu A_\mu + \bar{\chi} c + \bar{c} \chi + Rh). \quad (\text{A3})$$

We first make the change of variables $\bar{c}(x) \rightarrow \bar{c}(x) + \bar{\eta}(x)$. This yields the equation:

$$\partial_\mu \frac{\delta \Gamma}{\delta \bar{K}_\mu^a(x)} = \frac{\delta \Gamma}{\delta \bar{c}^a(x)}. \quad (\text{A4})$$

Deriving this equation with respect to $c^b(y)$ and taking the Fourier transform [our convention is $\tilde{f}(p) = \int d^d x \exp(ipx) f(x)$], we get:

$$\Gamma_{\bar{c}^a c^b}^{(2)}(p) = -ip_\mu \Gamma_{\bar{K}_\mu^a c^b}^{(2)}(p). \quad (\text{A5})$$

We moreover need the Slavnov-Taylor equation, which reads:

$$\int d^d x \left\{ \frac{\delta \Gamma}{\delta A_\mu^a(x)} \frac{\delta \Gamma}{\delta \bar{K}_\mu^a(x)} + \frac{\delta \Gamma}{\delta c^a(x)} \frac{\delta \Gamma}{\delta \bar{L}^a(x)} - ih^a(x) \frac{\delta \Gamma}{\delta \bar{c}^a(x)} + im^2 \frac{\delta \Gamma}{\delta h^a(x)} c^a(x) \right\} = 0. \quad (\text{A6})$$

We derive this expression with respect to $A_\nu^b(y)$ and $c^c(z)$ and take this expression at vanishing sources. Using the fact that the vacuum does not break the ghost number conservation, only two terms contribute and making the Fourier transform we get:

$$\Gamma_{A_\nu^b A_\mu^a}^{(2)}(p) \Gamma_{\bar{K}_\mu^a c^c}^{(2)}(p) = im^2 \Gamma_{A_\nu^b h^c}^{(2)}(p) = -im^2 p_\nu \delta^{bc}, \quad (\text{A7})$$

where we used the fact that the h sector is not renormalized.

Now, using the fact that $\Gamma_{A_\mu^a A_\nu^b}^{(2)}(p)$ is analytic at low momentum and behaves as $\delta^{ab} \delta_{\mu\nu} G^{-1}(0)$, and contracting Eq. (A7) with p_ν , we obtain at low energy:

$$G_B^{-1}(0) F_B^{-1}(0) = m_B^2, \quad (\text{A8})$$

where we have introduced the subscript B to recall that all this calculation was done (as emphasized at the beginning of the appendix) with bare quantities.

APPENDIX B: INFRARED BEHAVIOR OF THE FEYNMAN DIAGRAMS

In this appendix we study the IR corrections coming from higher order diagrams. Our aim is twofold. First we check that the regular IR behavior found at one-loop is not modified by higher order corrections. Second we study the IR behavior of the low-energy effective theory for the ghosts obtained by considering only a minimal number of gluon propagators (see Sec. IV E).

Consider first a generic diagram of the model (1). It has N_A external gluon legs, N_c external ghost/antighost legs, v_3 three-gluon vertices, v_4 four-gluon vertices, and v_c ghost-antighost-gluon vertices. Looking at the bare vertex, we see that each external antighost leg comes with an external momentum. In the following when we speak of diagrams, it is understood that these trivial external momenta dependences have been factorized.

Let us calculate the superficial degree of IR divergence ω of this diagram for vanishing external momenta, which characterize the IR behavior of the associated integrals. A negative superficial degree of IR divergence indicates that the corresponding diagram is IR divergent (at zero momenta). Each ghost propagator contributes -2 but the gluon propagators being massive do not contribute. The 3-point interactions being proportional to a momentum contribute $+1$ and each loop contributes d . Using textbook techniques [58], it is easy to prove that:

$$\omega \geq d - \frac{d}{2}N_A - \frac{d-1}{2}N_c + \frac{d}{2}v_3 + dv_4 + \frac{d-2}{2}v_c. \quad (\text{B1})$$

Observing that the prefactors of v_3 , v_4 , and v_c are positive in $d > 2$, we conclude that, at a fixed number of external legs, increasing the number of vertices suppresses the contributions in the IR. Moreover we check that the 2-point vertex functions at zero momenta are finite at all loops. The case $d \leq 2$ is different because increasing the number of ghost-gluon vertices does not improve (or even worsen for $d < 2$) the IR behavior. In this sense, $d = 2$ plays the role of an upper critical dimension.

The situation is, as expected, more favorable if we consider nonexceptional momentum configurations. Using the method described in [58], we find that the degree of IR divergence is:

$$\omega \geq \frac{d}{2}N_A + \frac{d-1}{2}N_c + \frac{d+2}{2}v_3 + dv_4 + \frac{d-2}{2}v_c, \quad (\text{B2})$$

where now N_A and N_c are the external soft legs of the diagram and v_3 , v_4 , and v_c are the number of vertices attached only to soft momenta. This expression is always positive for $d > 2$ but again $d = 2$ plays the role of an upper critical dimension.

We now come to the discussion of the IR behavior of the diagrams in the effective theory. We consider first diagrams with vanishing external momenta (as before, we first factorize the external momenta of the antighosts). As discussed in Sec. IV E, the ghosts interact via a 4-point vertex which behaves as the product of momenta of the antighosts. Denoting v_{4c} the number of such vertices in a diagram, we find the IR degree of divergence:

$$\omega = d - N_A - \frac{d-1}{2}N_c + (d-2)v_{4c}. \quad (\text{B3})$$

Again, we see that, at a fixed number of external legs, increasing the number of vertices suppresses the contributions in the IR and check that the 2-point vertex functions at zero momenta remain finite at higher loops. Using nonexceptional momentum configurations, we get:

$$\omega = \frac{d-1}{2}N_c + (d-2)v_{4c}, \quad (\text{B4})$$

which ensures that the diagrams are IR finite for $d \geq 2$.

-
- [1] V.N. Gribov, *Nucl. Phys.* **B139**, 1 (1978).
 [2] T.R. Morris, *Nucl. Phys.* **B573**, 97 (2000).
 [3] T.R. Morris, *J. High Energy Phys.* 12 (2000) 012.
 [4] T.R. Morris and O.J. Rosten, *Phys. Rev. D* **73**, 065003 (2006).
 [5] L. von Smekal, R. Alkofer, and A. Hauck, *Phys. Rev. Lett.* **79**, 3591 (1997).
 [6] R. Alkofer and L. von Smekal, *Phys. Rep.* **353**, 281 (2001).
 [7] D. Zwanziger, *Phys. Rev. D* **65**, 094039 (2002).
 [8] C.S. Fischer and R. Alkofer, *Phys. Rev. D* **67**, 094020 (2003).
 [9] J.C.R. Bloch, *Few-Body Syst.* **33**, 111 (2003).
 [10] A.C. Aguilar and A.A. Natale, *J. High Energy Phys.* 08 (2004) 057.
 [11] Ph. Boucaud *et al.*, *J. High Energy Phys.* 06 (2006) 001.
 [12] A.C. Aguilar and J. Papavassiliou, *Eur. Phys. J. A* **35**, 189 (2008).
 [13] A.C. Aguilar, D. Binosi, and J. Papavassiliou, *Phys. Rev. D* **78**, 025010 (2008).
 [14] P. Boucaud, J.P. Leroy, A. Le Yaouanc, J. Micheli, O. Pene, and J. Rodriguez-Quintero, *J. High Energy Phys.* 06 (2008) 099.
 [15] C.S. Fischer, A. Maas, and J.M. Pawłowski, *Ann. Phys. (N.Y.)* **324**, 2408 (2009).
 [16] J. Rodriguez-Quintero, *J. High Energy Phys.* 01 (2011) 105.
 [17] C. Wetterich, *Phys. Lett. B* **301**, 90 (1993).
 [18] J. Berges, N. Tetradis, and C. Wetterich, *Phys. Rep.* **363**, 223 (2002).
 [19] J.M. Pawłowski, D.F. Litim, S. Nedelko, and L. von Smekal, *Phys. Rev. Lett.* **93**, 152002 (2004).
 [20] C.S. Fischer and H. Gies, *J. High Energy Phys.* 10 (2004) 048.
 [21] D. Zwanziger, *Nucl. Phys.* **B323**, 513 (1989).
 [22] D. Zwanziger, *Nucl. Phys.* **B399**, 477 (1993).
 [23] M.A. Semenov-Tyan-Shanskii and V.A. Franke, *Zapiski Nauchnykh Seminarov Leningradskogo Otdeleniya Matematicheskogo Instituta im. V.A. Steklov AN SSSR* **120**, 159 (1982); [*J. Sov. Math.* **34**, 1999 (1986)].
 [24] D. Dudal, J.A. Gracey, S.P. Sorella, N. Vandersickel, and H. Verschelde, *Phys. Rev. D* **78**, 065047 (2008).
 [25] A. Cucchieri and T. Mendes, *Phys. Rev. Lett.* **100**, 241601 (2008); *Proc. Sci. QCD-TNT09* (2009) 026 [arXiv:1001.2584].
 [26] A. Cucchieri and T. Mendes, *Phys. Rev. D* **78**, 094503 (2008).
 [27] A. Cucchieri and T. Mendes, *Phys. Rev. D* **81**, 016005 (2010).

- [28] I. L. Bogolubsky *et al.*, *Phys. Lett. B* **676**, 69 (2009).
- [29] D. Dudal, O. Oliveira, and N. Vandersickel, *Phys. Rev. D* **81**, 074505 (2010).
- [30] A. Maas, *Phys. Rev. D* **75**, 116004 (2007).
- [31] D. Dudal, S.P. Sorella, N. Vandersickel, and H. Verschelde, *Phys. Lett. B* **680**, 377 (2009).
- [32] M. Tissier and N. Wschebor, *Phys. Rev. D* **82**, 101701 (2010).
- [33] G. Curci and R. Ferrari, *Nuovo Cimento Soc. Ital. Fis. A* **32**, 151 (1976).
- [34] P.O. Bowman *et al.*, *Phys. Rev. D* **76**, 094505 (2007).
- [35] A. Cucchieri, T. Mendes, and A.R. Taurines, *Phys. Rev. D* **71**, 051902 (2005).
- [36] H. Verschelde, K. Knecht, K. Van Acoleyen, and M. Vanderkelen, *Phys. Lett. B* **516**, 307 (2001).
- [37] R.E. Browne and J.A. Gracey, *J. High Energy Phys.* **11** (2003) 029.
- [38] G. Parisi and R. Petronzio, *Phys. Lett. B* **94**, 51 (1980).
- [39] J.M. Cornwall, *Phys. Rev. D* **26**, 1453 (1982).
- [40] A.A. Natale, *Proc. Sci. QCD-TNT09* (2009) 031 [arXiv:0910.5689].
- [41] J.M. Cornwall, *Nucl. Phys.* **B157**, 392 (1979).
- [42] C. Becchi, A. Rouet, and R. Stora, *Commun. Math. Phys.* **42**, 127 (1975); *Ann. Phys. (N.Y.)* **98**, 287 (1976).
- [43] I. V. Tyutin, Report No. LEBEDEV-75-39.
- [44] J. de Boer, K. Skenderis, P. van Nieuwenhuizen, and A. Waldron, *Phys. Lett. B* **367**, 175 (1996).
- [45] F. Delduc and S.P. Sorella, *Phys. Lett. B* **231**, 408 (1989).
- [46] M. Tissier and N. Wschebor, *Phys. Rev. D* **79**, 065008 (2009).
- [47] In Ref. [46], a different but equivalent form of the action has been employed that makes manifest the symmetry $c \leftrightarrow \bar{c}$.
- [48] D. Dudal, H. Verschelde, and S.P. Sorella, *Phys. Lett. B* **555**, 126 (2003).
- [49] J.C. Taylor, *Nucl. Phys.* **B33**, 436 (1971).
- [50] N. Wschebor, *Int. J. Mod. Phys. A* **23**, 2961 (2008).
- [51] J.A. Gracey, *Phys. Lett. B* **552**, 101 (2003).
- [52] P. Boucaud, F. De Soto, J.P. Leroy, A. Le Yaouanc, J. Micheli, O. Pene, and J. Rodriguez-Quintero, *Phys. Rev. D* **79**, 014508 (2009).
- [53] S. Weinberg *The Quantum Theory of Fields* (Cambridge University Press, Cambridge, England, 1995), Vol. 1, Chap. 8, p. 609.
- [54] We show in Appendix B that this effective field theory is also IR safe for nonexceptional momenta for $d > 2$.
- [55] G. Grinstein and A. Luther, *Phys. Rev. B* **13**, 1329 (1976).
- [56] D. Khmel'nitskii, *Zh. Eksp. Teor. Fiz.* **68**, 1960 (1975); [*Sov. Phys. JETP* **41**, 981 (1976)].
- [57] C. Jayaprakash and H.J. Katz, *Phys. Rev. B* **16**, 3987 (1977).
- [58] C. Itzykson and J.B. Zuber, *International Series in Pure and Applied Physics* (McGraw-Hill, New York, 1980), p. 705.